Multifunctional Magnetic Nanocomposite Encapsulant for Electromagnetic Interference Shielding in Power Electronics

Hayden Carlton
Mechanical Engineering Department,
University of Arkansas,
700 Research Center Building,
Fayetteville, AR 72701

Ange Iradukunda
Mechanical Engineering Department,
University of Arkansas,
700 Research Center Building,
Fayetteville, AR 72701

Asif Imran
Department of Electrical and Computer Engineering,
Stony Brook University,
100 Nicolls Road,
Stony Brook, NY 11794-2350

Sarah Myane
Fay Jones School of Architecture and Design,
University of Arkansas,
120 Vol Walker Hall,
Fayetteville, AR 72701

Noah Akey
NorthWest Arkansas Community College (NWACC),
1 College Drive,
Bentonville, AR 72712

Fang Luo
Department of Electrical and Computer Engineering,
Stony Brook University,
100 Nicolls Road,
Stony Brook, NY 11794-2350

David Huitink[1]
Mechanical Engineering Department,
University of Arkansas,
700 Research Center Building,
Fayetteville, AR 72701
e-mail: dhuitin@uark.edu

As power densities and switching frequencies dramatically increase in wide bandgap power electronics, electromagnetic interference (EMI) increasingly impacts power conversion efficiency, and reliability, which requires mitigation for effective operation. Herein, we propose a nanocomposite encapsulant created by directly incorporating magnetic iron oxide nanoparticles into a silicone matrix for the purpose of EMI shielding. The addition of small amounts of particles to the silicone resulted in a 1.7 dBμV drop in EMI intensity; however, the addition of the iron oxide reduced the dielectric breakdown strength of the silicone matrix by 83% with respect to concentration. Further efforts to optimize the dielectric properties of the nanocomposites with respect to the nanoparticle loading are necessary to directly apply this technology; yet the results indicate that magnetic nanocomposites could be a potential avenue toward mitigating EMI in power devices. [DOI: 10.1115/1.4053642]

Introduction

Electromagnetic interference (EMI) continues to be a pertinent issue with the development and maintenance of modern wide bandgap power electronic systems. The transmission of these signals can either be through radiation or conduction, and they are especially prevalent in high power density devices, due to the high rate of voltage $(\frac{dV}{dt})$ and current $(\frac{di}{dt})$ change over time associated with the switching of semiconductors [1]. Parasitic couplings contribute largely to the generation of EMI in power electronics packages [2]; among the more common type of EMI is common mode noise, where parasitic capacitances found within the packaging generate leakage currents [3].

A large percentage of research centers on EMI mitigation, typically by introducing passive components or active EMI filters within the circuitry [4,5]. These filtering components, while effective, often reduce overall power density by increasing the package size. Another methodology consists of introducing a shielding material around or near the package to inhibit the transmission of EMI [6,7]. Early forms of shielding utilized metallic compounds. Being excellent conductors of electric currents, metal enclosures easily absorb and reflect EMI; however, despite their effectiveness, their high density and poor flexibility limited the usage of metals significantly in modern electronics packages [8]. Alternatively, researchers and manufacturers began investigating polymer-based shields. One such example in literature utilized a polymer-based heat sink to reduce common-mode noise [9]. Unlike with metal shields, where conductivity drives the shielding effectiveness, permittivity plays a larger role in EMI shielding with low conductivity materials, like polymers; micron and nano-sized conductive additives allow for polymeric materials to have EMI-reducing functionality by increasing their permittivity, thus enhancing electrical energy storage [10,11]. Specific examples from the literature include the incorporation of carbon-based materials [12–14] as well as stainless steel fibers [15].

Along with conductive additives, the usage of ferro/ferrimagnetic additives to polymeric compounds continues to be a recurring concept in literature [16]. The recent review by Shukla et al. presents an encompassing synopsis of EMI shielding with iron ingredients, where the shielding efficiency is largely dependent on the permeability of the material [17]. In some cases, iron oxide nanoparticles (IONPs) are utilized for shielding purposes as opposed to elemental iron, due to their colloidal stability on the nanoscale and widespread usage in the scientific community. Their properties and EMI shielding performance can even be tuned through modifying their relative size [18]. Shielding materials such as polymers enhanced with ferromagnetic particulate not only reduce the need for EMI filtering but also increase the overall power density by eliminating bulky EMI shielding from the packaging structure. Herein, IONP/silicone nanocomposites are introduced for use as a multifunctional EMI-shielding encapsulant for use with switching power electronics, with associated materials testing relevant to power module incorporation.

Nanocomposite Fabrication

Magnetite (Fe_3O_4) IONPs were acquired through U.S. Research Nanomaterial, Inc., Houston, TX, in the form of a dry powder, due to its relatively high saturation magnetization and susceptibility. Upon receipt, the IONP powder underwent X-ray diffraction (XRD) in order to verify the chemical composition provided by

[1]Corresponding author.

Contributed by the Electronic and Photonic Packaging Division of ASME for publication in the Journal of Electronic Packaging. Manuscript received March 29, 2021; final manuscript received January 13, 2022; published online February 16, 2022. Assoc. Editor: Jaeho Lee.

the manufacturer. The sample possessed peaks characteristic of the iron oxide structures magnetite and maghemite (γ-Fe_2O_3), which was verified via the RRUFF database for magnetite R061111 [19]. Full-Width Half Max measurements at the principle (311) peak indicate that the size range of the measured structures lies within the nanosize regime.

The encapsulant used for this study consisted of a two-part molding silicone (Smooth-On Mold Max 40), which possesses a high dielectric strength, and is commonly used as the base material in commercial insulation gels. Each sample was mixed at a 1:10 ratio of curing agent to bulk silicone; IONPs at increasing concentrations were then mixed into the silicone using a mechanical stirrer. The addition of the iron oxide particles resulted in a black appearance, with the original green color no longer visible at a concentration above 7 mg/mL. After thoroughly mixing and an overnight cure time, the samples achieved a visually homogenous distribution of nanoparticles, as shown in Fig. 1.

Electromagnetic Interference Shielding Analysis

In an effort to determine the EMI shielding effectiveness of the nanocomposite material, radiated noise was measured with a TEKBOX electromagnetic compatibility (EMC) probe set and a spectrum analyzer. The emitted noise was created via a function generator passing a square wave current at 600 kHz through a single copper trace in a printed circuit board (PCB); a speed in the kilohertz regime mimicked the switching speed used commonly in power electronics. Using a single trace ensured that the emitted EMI originated from a single controlled source, which allowed for the shielding effect of the nanocomposite to be isolated. The circular nanocomposite sample was placed directly on top of the single trace to mimic an encapsulant, as shown in Fig. 2. The spectrum analyzer measured radiated EMI within the range of 20–100 MHz.

To start, the spectrum analyzer, in the orientation shown in Fig. 2, measured the radiated EMI in two separate conditions: (1) bare PCB without added nanocomposite, (2) PCB with 140 mg/mL nanocomposite added. Each condition was measured three separate times and averaged in order to establish adequate measurement statistics. Figure 3 displays the averaged EMI spectra for the two conditions within the range of 20–100 MHz. It becomes apparent that the addition of the nanocomposite provides a slight dampening effect on the radiated EMI within the tested range of frequencies; one of the peaks highlighted in Fig. 3 indicated as much as a 0.5 dBμV drop.

While the dampening effect observed in Fig. 3 seems rather small, we believe it to be commensurate given the relatively small amount of nanomaterial added to the silicone (2.4 vol. % Fe_3O_4 at

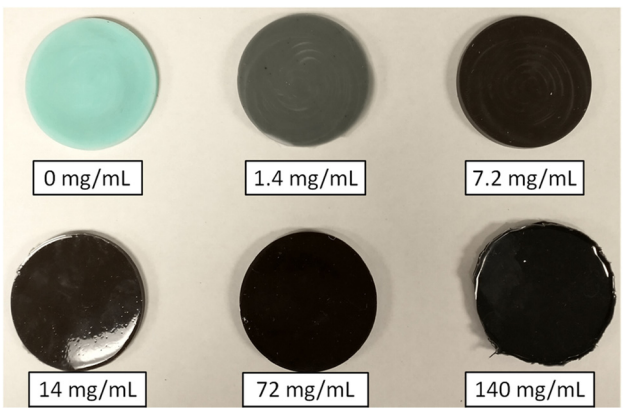

Fig. 1 Sample appearances with varying IONP concentration. The first sample showcases unmodified silicone; as IONPs were added to the silicone matrix, the samples become progressively darker. The distribution in each sample appeared to be homogenous in each sample with no major clusters.

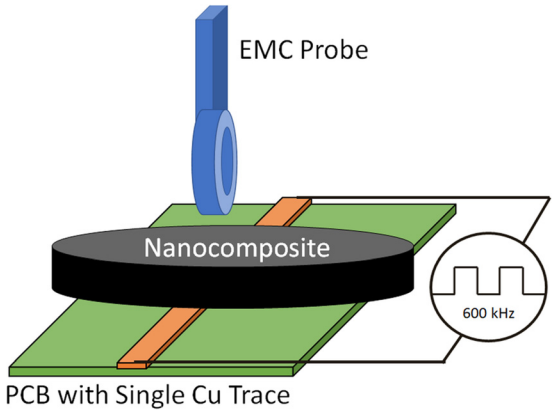

Fig. 2 Placement of nanocomposite and EMC probe with respect to the PCB. The nanocomposite is laying parallel to the PCB surface, as to mimic an encapsulant, and the probe is orthogonal to the H field produced by the trace, to maximize detection.

140 mg/mL). It can be inferred that increasing the concentration of magnetic material would only stand to further improve the EMI shielding capability of the encapsulating material. To investigate this notion, the same experiment was performed with nanocomposites at higher concentrations of iron oxide: 280, 420, and 560 mg/mL (4.8, 7.2, and 9.6 vol. %, respectively). However, to analyze the EMI dampening effects across the entire measured spectrum, the magnitude of each peak must be taken into consideration, not just a single peak. Using MATLAB, the peaks from the each spectrum were identified, and their magnitudes were recorded as a vector (p_1, p_2,…, p_n). From here, the Euclidian norm (two-norm) (Eq. (1)) for each spectrum was calculated to encompass the magnitude of all the peaks within the spectrum in a single value. The resulting calculation and EMI reduction can be seen in Table 1.

$$\|p\|_2 = \sqrt{p_1^2 + p_2^2 + \cdots + p_n^2} \tag{1}$$

When considering the entire spectra, the calculations shown in Table 1 indicate that increasing the concentration of the nanoparticles results in a greater reduction in EMI. By observing this trend, increasing the concentration of iron oxide in the nanocomposite should continue to improve EMI reduction; however, there most certainly exists a concentration upper limit, which would

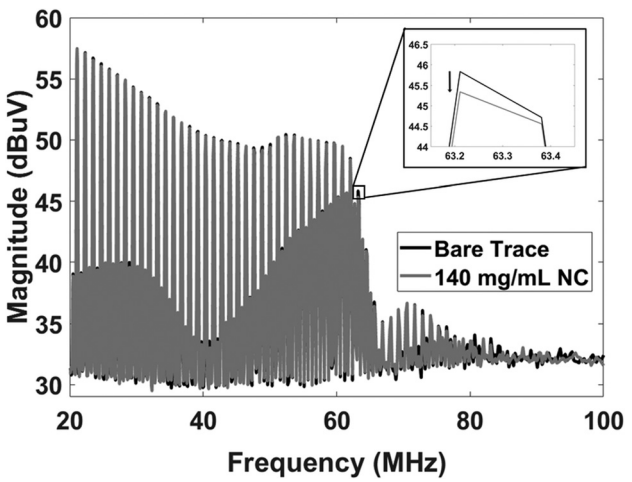

Fig. 3 Entire spectrum emitted from the single trace PCB. The zoomed in portion of the graph displays a specific instance where the addition of the nanocomposite reduced the magnitude of the EMI by as much as 0.5 dBμV.

Table 1 EMI reduction across the measured spectrum (20–100 MHz) for samples at higher concentrations

Concentration of Fe_3O_4	Two-norm of spectra (Eq. (1))	EMI reduction
Bare PCB	395.52 dBμV	—
140 mg/mL	395.42 dBμV	0.1 dBμV
280 mg/mL	394.42 dBμV	1.1 dBμV
420 mg/mL	394.62 dBμV	0.9 dBμV
560 mg/mL	393.79 dBμV	1.73 dBμV

Each sample is then compared to the bare copper condition (0 mg/mL).

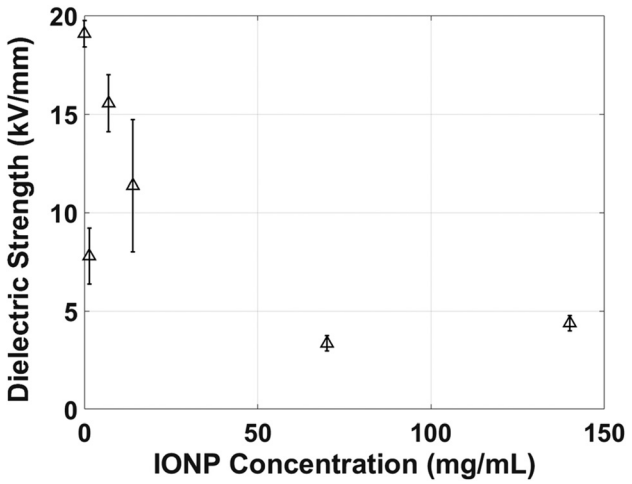

Fig. 4 Dielectric strength with respect to IONP concentration. Adding even small amount of IONPs resulted in a drastic decrease in dielectric strength. At higher concentrations, the decrease appears to be much more gradual.

result in degradation of the bulk silicone material properties, i.e., the maximum amount of iron oxide that could be added before the silicone began to break down. In this study, this upper limit was not investigated, but studies in literature have tested nanocomposites with concentrations approaching 50 vol. % [20,21]. As the concentration of the nanocomposite increases and the iron oxide nanoparticles become the majority species, it may degrade the mechanical, thermal, and electrical properties of the bulk silicone. In the case of power electronics packaging, silicone is revered for its dielectric strength, but the addition of nanoparticles to the silicone polymer could possibly introduce conduction paths, thus significantly reducing dielectric strength and inhibiting its functionality as an encapsulant.

Dielectric Breakdown Analysis

The dielectric strength of the nanocomposites was measured using a custom-built tester, which consisted of two electrodes (one grounded) separated by the nanocomposite sample. The applied voltage was supplied by a Valhalla Scientific 5880 A High Voltage Potentiostat (max rating of 7 kV). Figure 4 indicates an inverse relationship between these two parameters (i.e., dielectric strength decreases with IONP concentration). Bulk silicone

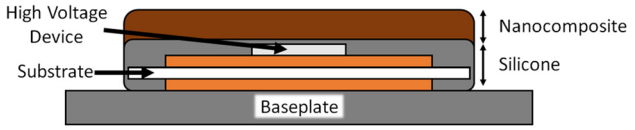

Fig. 5 An illustrated example of how the nanocomposite could be implemented without risking dielectric failure

possessed the highest strength at 19 kV/mm, while at higher concentrations (>50 mg/mL), the strength decreased by nearly 83% to 3.3 kV/mm. From a material perspective, dielectric strength represents the main limiting factor when utilizing IONP additives in silicone. The presence of nanoparticles within the silicone matrix results in an increased likelihood of conduction path formation for electrons, which is more prevalent at higher concentrations [22].

Potential Improvements to Dielectric Strength

While the presence of IONPs has the potential to interfere with the produced EMI fields, its obvious dampening effect on dielectric performance must not be overlooked. Testing results indicate that even at small concentrations of IONPs, dielectric strength is reduced; however, commensurate decreases in the dielectric strength of nanocomposites have occurred in literature (Table 2) with both Ag and barium titanate (BT) nanoparticles.

Consider a comparison between the study involving BT nanoparticles in a poly(vinylidene fluoride) (PVDF) matrix and this study (iron oxide nanoparticles in a silicone matrix). The BT nanoparticle surface-modifying agent (tetrafluorophthalic acid) essentially functionalized the nanoparticles to achieve better compatibility with the surrounding PVDF matrix, resulting in better nanoparticle dispersion. In addition to introducing stronger chemical bonding between the nanoparticles and filler, the surface agent acted as a layer of passivation, which limited the transmission of electric charge [24]. As a result, the surface modification improved the dielectric strength of the nanocomposite. In the case of this study, the IONPs visually appeared to have decent dispersion throughout the silicone; however, dried particles are prone to aggregation, where the nanosized fillers combine to form defects in the silicone structure on the micron level and reduce the dielectric strength even further [25]. Based on the rapid decrease in dielectric strength with respect to IONP concentration (Fig. 4), it can be inferred that the lack of capping agent within the IONP powder facilitated poor bonding with the surrounding silicone matrix, which in turn dissuaded effective dispersion within the silicone, promoted IONP aggregation, created conduction paths, and negatively impacted the dielectric strength. Chemically modifying the surface of the dispersed nanoparticles is an effective methodology to encourage chemical bonding between the nanoparticle filler and matrix material within a nanocomposite [26], which ultimately increases the dielectric strength of the material.

Conclusions and Implications for Power Electronics

To conclude, the addition of magnetic nanoparticles to an encapsulant has the potential to serve as a passive means of radiated EMI mitigation. At the highest concentration tested, 9.6 vol. %, the nanocomposite dampened the measured EMI by 1.7 dBμV; however, the addition of iron oxide nanoparticles in the silicone

Table 2 Examples of nanocomposites in literature and how the nanoparticle additives impacted dielectric strength

Matrix	Filler nanoparticles	Volume fraction	Decrease in dielectric strength	References
Silicone	Uncapped Fe_3O_4	0.024	83%	—
Epoxy	Ag-core/organic shell	0.2	97%	[23]
PVDF	Untreated $BaTiO_3$	0.1	30%	[24]
PVDF	Treated $BaTiO_3$	0.1	19%	[24]

matrix significantly degraded the dielectric strength of the nanocomposite. In the case of this study, the dielectric strength was reduced by over 83% with just 2.4 vol. % iron oxide. Being prone to dielectric failure during normal operation would limit the usage of this material locally in a high voltage environment. If this nanocomposite is to be used, designers must be mindful of the voltage differentials present within the system, such as those between wire bonds or neighboring solder balls. A potential remedy for this issue would be to layer the nanocomposite encapsulant directly on top of unmodified encapsulants (without nanosized additives), as seen illustrated in Fig. 5.

Since the nanocomposite possesses low dielectric strength, unmodified silicone is first used to encapsulate the device and interconnects, or other areas of high potential. The nanocomposite is then introduced as a secondary layer on top of the existing silicone. Encapsulating the device this way would allow the nanocomposite to be in close proximity to the devices without exacerbating the risk of dielectric failure. A potential avenue for future work could be to optimize this two-layer encapsulant structure in terms of layer thickness and EMI shielding effectiveness. Nanocomposites as passive EMI-absorbing encapsulants represents a point of potential advancement in the field of power electronics, which could prove useful in improving overall device function without sacrificing module power density.

Acknowledgment

The authors would like to thank the University of Arkansas for providing the facilities and resources to support this project, specifically the Young Scholar's program under the POETS-ERC. We also would like to thank the High Density Electronics Center for usage of the XRD and Dielectric Testing facilities. Any opinions, finding, and conclusions or recommendations expressed in this material are those of the author(s) and do not necessarily reflect the views of the National Science Foundation.

Funding Data

- Partially supported through the POETS-ERC, under the National Science Foundation (Grant No. 2014-00555-04; Funder ID: 10.13039/100000001).

Nomenclature

EMC = electromagnetic compatibility
EMI = electromagnetic interference
IONP = iron oxide nanoparticles
PCB = printed circuit board
PVDF = poly(vinylidene fluoride)
XRD = X-ray diffraction

References

[1] Costa, F., and Magnon, D., 2005, "Graphical Analysis of the Spectra of EMI Sources in Power Electronics," IEEE Trans. Power Electron., **20**(6), pp. 1491–1498.
[2] Wang, S., Lee, F. C., Chen, D. Y., and Odendaal, W. G., 2004, "Effects of Parasitic Parameters on EMI Filter Performance," IEEE Trans. Power Electron., **19**(3), pp. 869–877.
[3] Wang, S., and Lee, F. C., 2010, "Analysis and Applications of Parasitic Capacitance Cancellation Techniques for EMI Suppression," IEEE Trans. Ind. Electron., **57**(9), pp. 3109–3117.
[4] Murata, Y., Takahashi, K., Kanamoto, T., and Kubota, M., 2017, "Analysis of Parasitic Couplings in EMI Filters and Coupling Reduction Methods," IEEE Trans. Electromagn. Compat., **59**(6), pp. 1880–1886.
[5] Takahashi, K., Murata, Y., Tsubaki, Y., Fujiwara, T., Maniwa, H., and Uehara, N., 2019, "Mechanism of Near-Field Coupling Between Noise Source and EMI Filter in Power Electronic Converter and Its Required Shielding," IEEE Trans. Electromagn. Compat., **61**(5), pp. 1663–1672.
[6] Xu, C. D., Cheng, K. W. E., Zou, Y., Ho, H. F., and Wang, X. L., and 2016, "A Polymer Bonded Gridded Box EMI Shielding Method Based on FEM for High Speed Railway," International Symposium on Electrical Engineering (ISEE), Hong Kong, China, Dec. 14, p. 4.
[7] Yang, Y. C., Huang, D. C., Lee, F. C., and Li, Q., and 2013, "Transformer Shielding Technique for Common Mode Noise Reduction in Isolated Converters," IEEE Energy Conversion Congress and Exposition (ECCE), Denver, CO, Sept. 15–19, pp. 4149–4153.
[8] Geetha, S., Kumar, K. K. S., Rao, C. R. K., Vijayan, M., and Trivedi, D. C., 2009, "EMI Shielding: Methods and Materials-A Review," J. Appl. Polym. Sci., **112**(4), pp. 2073–2086.
[9] Whitt, R., Huitink, D., Hudson, S., Nafis, B., Yuan, Z., Narayanasamy, B., Deshpande, A., Luo, F., Imran, A., Clarke, Z., and Smith, S., 2019, "Additive Manufactured, Low EMI, Non-Metallic Convective Heat Spreader Design and Optimization," ASME Paper No. IPACK2019-6442.
[10] Ganguly, S., Bhawal, P., Ravindren, R., and Das, N. C., 2018, "Polymer Nanocomposites for Electromagnetic Interference Shielding: A Review," J. Nanosci. Nanotechnol., **18**(11), pp. 7641–7669.
[11] Jiang, D. W., Murugadoss, V., Wang, Y., Lin, J., Ding, T., Wang, Z. C., Shao, Q., Wang, C., Liu, H., Lu, N., Wei, R. B., Subramania, A., and Guo, Z. H., 2019, "Electromagnetic Interference Shielding Polymers and Nanocomposites-A Review," Polym. Rev., **59**(2), pp. 280–337.
[12] Chung, D. D. L., 2001, "Electromagnetic Interference Shielding Effectiveness of Carbon Materials," Carbon, **39**(2), pp. 279–285.
[13] Thomassin, J. M., Jerome, C., Pardoen, T., Bailly, C., Huynen, I., and Detrembleur, C., 2013, "Polymer/Carbon Based Composites as Electromagnetic Interference (EMI) Shielding Materials," Mater. Sci. Eng. R-Rep., **74**(7), pp. 211–232.
[14] Sankaran, S., Deshmukh, K., Ahamed, M. B., and Pasha, S. K. K., 2018, "Recent Advances in Electromagnetic Interference Shielding Properties of Metal and Carbon Filler Reinforced Flexible Polymer Composites: A Review," Compos. Part A Appl. Sci. Manuf., **114**, pp. 49–71.
[15] Chen, C. S., Chen, W. R., Chen, S. C., and Chien, R. D., 2008, "Optimum Injection Molding Processing Condition on EMI Shielding Effectiveness of Stainless Steel Fiber Filled Polycarbonate Composite," Int. Commun. Heat Mass Transfer, **35**(6), pp. 744–749.
[16] Azadmanjiri, J., Hojati-Talemi, P., Simon, G. P., Suzuki, K., and Selomulya, C., 2011, "Synthesis and Electromagnetic Interference Shielding Properties of Iron Oxide/Polypyrrole Nanocomposites," Polym. Eng. Sci., **51**(2), pp. 247–253.
[17] Shukla, V., 2019, "Review of Electromagnetic Interference Shielding Materials Fabricated by Iron Ingredients," Nanoscale Adv., **1**(5), pp. 1640–1671.
[18] Bayat, M., Yang, H., and Ko, F., 2018, "Effect of Iron Oxide Nanoparticle Size on Electromagnetic Properties of Composite Nanofibers," J. Compos. Mater., **52**(13), pp. 1723–1736.
[19] Lafuente, B., Downs, R. T., Yang, H., and Stone, N., 2015, "The Power of Databases: The RRUFF Project," *Highlights in Mineralogical Crystallography*, W. De Gruyter, Berlin, Germany, pp. 1–30.
[20] Novakova, A. A., Lanchinskaya, V. Y., Volkov, A. V., Gendler, T. S., Kiseleva, T. Y., Moskvina, M. A., and Zezin, S. B., 2003, "Magnetic Properties of Polymer Nanocomposites Containing Iron Oxide Nanoparticles," J. Magn. Magn. Mater., **258–259**, pp. 354–357.
[21] Evans, B. A., Fiser, B. L., Prins, W. J., Rapp, D. J., Shields, A. R., Glass, D. R., and Superfine, R., 2012, "A Highly Tunable Silicone-Based Magnetic Elastomer With Nanoscale Homogeneity," J. Magn. Magn. Mater., **324**(4), pp. 501–507.
[22] Liu, Z. L., Peng, W. X., Zare, Y., Hui, D., and Rhee, K. Y., 2018, "Predicting the Electrical Conductivity in Polymer Carbon Nanotube Nanocomposites Based on the Volume Fractions and Resistances of the Nanoparticle, Interphase, and Tunneling Regions in Conductive Networks," Rsc Adv., **8**(34), pp. 19001–19010.
[23] Shen, Y., Lin, Y. H., Li, M., and Nan, C. W., 2007, "High Dielectric Performance of Polymer Composite Films Induced by a Percolating Interparticle Barrier Layer," Adv. Mater., **19**(10), pp. 1418–1422.+.
[24] Yu, K., Niu, Y. J., Xiang, F., Zhou, Y. C., Bai, Y. Y., and Wang, H., 2013, "Enhanced Electric Breakdown Strength and High Energy Density of Barium Titanate Filled Polymer Nanocomposites," J. Appl. Phys., **114**(17), p. 174107.
[25] Barber, P., Balasubramanian, S., Anguchamy, Y., Gong, S., Wibowo, A., Gao, H., Ploehn, H. J., and Zur Loye, H. C., 2009, "Polymer Composite and Nanocomposite Dielectric Materials for Pulse Power Energy Storage," Materials, **2**(4), pp. 1697–1733.
[26] Nelson, J. K., 2010, "Background, Principles and Promise of Nanodielectrics," *Dielectric Polymer Nanocomposites*, J. K. Nelson, ed., Springer, Boston, MA, p. 368.